*Journal of Sound and Vibration* (1999) **219**(3), 503–524
*Article No*. jsvi.1998.1904, available online at http://www.idealibrary.com.on IDEAL

# AN INTERPRETIVE METHOD FOR MOVING FORCE IDENTIFICATION

T. H. T. CHAN, S. S. LAW AND T. H. YUNG

*Department of Civil and Structural Engineering*,
*The Hong Kong Polytechnic University*, *Hung Hom*, *Kowloon*, *Hong Kong*

AND

X. R. YUAN

*Department of Communication Engineering*, *Shijiazhuang Railway Institution*,
*Shijiazhuang*, *Hebei*, *People's Republic of China*

(*Received September* 1997, *and in final form* 30 *July* 1998)

Dynamic load data have been valuable for bridge and pavement design. Traditional ways to acquire truck axle and gross weight information are expensive and subject to bias, and this has led to the development of Weigh-in-Motion (WIM) techniques. Most of the existing WIM systems have been developed to measure only the static axle loads. This paper aims to introduce a method to identify moving dynamic loads on bridges using the bridge responses caused by such loads. A closed-form solution can be obtained to identify moving constant loads, while numerical methods must be used to identify the time-varying moving loads. The set of equations that leads to the solution is based on Euler's equation of beams. A two-axle vehicle model is developed to generate the theoretical responses and the corresponding interactive moving forces. Studies were carried out to check whether the proposed method could recover the original interactive moving forces and the method was found to be feasible.



## 1. INTRODUCTION

The truck axle and gross weight information have applications in areas such as the structural and maintenance requirements of pavements and bridges, and road funding studies. Moses [1] states that these can be incorporated in safety factors to achieve more uniform risk against premature fatigue cracking. However, stopping and weighing vehicles, for instance, by weighbridge or loadometer, is not practical. It is not only expensive but also subject to bias. More often this survey data has obvious inconsistencies. Drivers of overweight vehicles learn about the tests and try to avoid the test stations because of the fear of penalty. It seems that the only way to avoid this is to monitor weights all the time and use some undetectable weigh-in-motion stations. As a result, there has been considerable research and testing going on worldwide since the late 60s and early 70s on equipment and schemes for weighing vehicles at highway speed, e.g., references

0022–460X/99/030503 + 22 $30.00/0 

[2–8]. Recently, two research activities, namely, COST 323 and WAVE, were carried out in Europe [9, 10]. These Weigh-in-Motion (WIM) systems can be categorised into two types, namely the road-surface system and the under-structure system [11].

The above systems measure only the equivalent static loads and not the peak dynamic wheel loads or the timewise dependence of these loads. However, the dynamic response of a bridge can be significant and Cebon [12] concludes that the dynamic wheel loads may increase road surface damage by a factor of 2 to 4 over that due to static wheel loads. For this reason the studies of dynamic wheel loads and ways to measure them had always been of interest. The dynamic wheel loads have been described in different terminology—as pavement loads or tyre forces or contact forces. Basically, all of them refer to the dynamic variation of the interactive forces exerted from the axle and acting on the contact surfaces. Three systems have been used at present to acquire such data: (1) Tyre Pressure Transducer System; (2) Strain-Gauged Axle Housing Transducer System; (3) Wheel Force Transducer System.

Whittemore *et al*. [13] and Cantieni [14] have separately given a summary of the above three systems. These systems are subject to bias because they all use instrumented vehicles to measure dynamic axle loads. These all prompt the need to develop a system to measure the dynamic interaction forces using an unbiased random sample of vehicles.

O'Connor and Chan [15] have developed a system to measure such dynamic forces, in which a bridge is modelled as an assembly of lumped masses interconnected by massless elastic beam elements. Law *et al*. [16, 17] adopted a different approach to identify the moving force based on system identification.

This paper introduces another method to identify moving dynamic forces. This method is similar to that developed by O'Connor and Chan [15] but uses Euler's equation for beams to model the bridge deck in the interpretation of dynamic loads crossing the deck. There are numerous reports on using Euler's beam to study bridge–vehicle interaction e.g., references [18–23]. They all concentrate on the investigation of bridge dynamic responses brought about by moving loads. The present study is an inverse study in which the Euler beam associated with modal analysis is used to identify moving loads from bridge responses. A simple two-axle vehicle model is used to generate the theoretical responses using the method developed by O'Connor and Chan [15] and the corresponding interactive forces. The proposed interpretive method then uses this response to identify the loads. The loads are then compared with the generated interactive forces from the vehicle model as an independent check on the proposed method.

## 2. THEORY

### 2.1. EQUATION OF MOTION

Referring to Figure 1, consider a load $P$ moving at a speed $c$ on a simply supported bridge deck with a span length $L$, constant stiffness $EI$, constant mass per unit length $\mu$ and viscous damping ratio $C$.

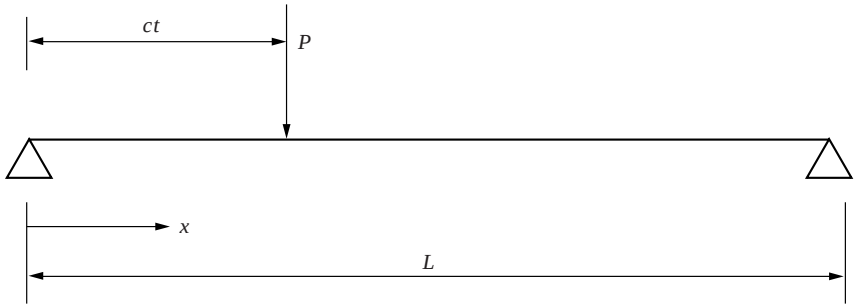


Figure 1. Moving load on an Euler beam.

By modelling the bridge deck as an Euler beam [24], the differential equation on the deflection of the beam is given as:

$$\mu \frac{\partial^2 v(x,t)}{\partial t^2} + C \frac{\partial v(x,t)}{\partial t} + EI \frac{\partial^4 v(x,t)}{\partial x^4} = \delta(x - ct)P, \tag{1}$$

where $v(x, t)$ is the beam deflection at point $x$ and time $t$ and $\delta(x)$ is the Dirac (impulse, or delta) function.

The boundary conditions for equation (1) are

$$v(0,t) \qquad v(L,t) = 0 \qquad \left.\frac{\partial^2 v(x,t)}{\partial x^2}\right|_{x=0} = 0 \qquad \left.\frac{\partial^2 v(x,t)}{\partial x^2}\right|_{x=L} = 0$$

and

$$v(x,0) = 0 \qquad \left.\frac{\partial v(x,t)}{\partial t}\right|_{t=0} = 0.$$

If the $i$th mode shape function of the beam is $\sin(i\pi x/L)$, then the solution of equation (1) takes the form

$$v = \sum_{i=1}^{\infty} \sin\frac{i\pi x}{L} \cdot V_i(t), \tag{2}$$

where $V_i(t)$, $(i = 1, 2, \ldots)$ are the modal displacements.

After substituting equation (2) into equation (1), each term of equation (1) is multiplied by the mode shape function $\sin(j\pi x/L)$ $(j = 1, 2, \ldots)$. The resultant equation is then integrated with respect to $x$ between 0 and $L$. Using the boundary conditions and the properties of the Dirac function, the following equation is obtained:

$$\ddot{V}_j(t) + 2\zeta_j \omega_{(j)} \dot{V}_j(t) + \omega_{(j)}^2 V_j(t) = \frac{2P}{\mu L} \sin\frac{j\bar{x}\pi}{L} \qquad j = 1, 2, \ldots, \infty, \tag{3}$$

where

$$\omega_{(j)}^2 = \frac{j^4\pi^4}{L^4}\frac{EI}{\mu}, \qquad \zeta_{(j)} = \frac{C}{2\mu\omega_{(j)}}$$

at the $j$th mode and $\bar{x}$ is the distance of the axle away from the bridge.

If there are $n$ moving loads on the beam, equation (3) can be written as

$$\begin{bmatrix} V_1 \\ \ddot{V}_2 \\ \vdots \\ \ddot{V}_n \end{bmatrix} + \begin{bmatrix} 2\zeta_1\omega_1\dot{V}_1 \\ 2\zeta_2\omega_2\dot{V}_2 \\ \vdots \\ 2\zeta_n\omega_n\dot{V}_n \end{bmatrix} + \begin{bmatrix} \omega_1^2 V_1 \\ \omega_2^2 V_2 \\ \vdots \\ \omega_n^2 V_n \end{bmatrix}$$

$$= \frac{2}{\mu L}\begin{bmatrix} \sin\frac{\pi(ct-\hat{x}_1)}{L} & \sin\frac{\pi(ct-\hat{x}_2)}{L} & \cdots & \sin\frac{\pi(ct-\hat{x}_k)}{L} \\ \sin\frac{2\pi(ct-\hat{x}_1)}{L} & \sin\frac{2\pi(ct-\hat{x}_2)}{L} & \cdots & \sin\frac{2\pi(ct-\hat{x}_k)}{L} \\ \vdots & \vdots & \vdots & \vdots \\ \sin\frac{n\pi(ct-\hat{x}_1)}{L} & \sin\frac{n\pi(ct-\hat{x}_2)}{L} & \cdots & \sin\frac{n\pi(ct-\hat{x}_k)}{L} \end{bmatrix}\begin{bmatrix} P_1 \\ P_2 \\ \vdots \\ P_k \end{bmatrix}, \quad (4)$$

in which $\hat{x}_k$ is the distance between the $k$th load and the first load, and $\hat{x}_1 = 0$. Therefore, the modal displacements can be obtained by solving equation (4). If equation (2) is expressed in a matrix form, i.e.,

$$v = \begin{bmatrix} \sin\frac{\pi x}{L} & \sin\frac{2\pi x}{L} & \cdots & \sin\frac{n\pi x}{L} \end{bmatrix}[V_1 \quad V_2 \quad \cdots \quad V_n]^T, \quad (5)$$

the displacements and accelerations on the beam at $x = x_1, x_2, \ldots, x_l$ can be calculated by using equations (6) and (7), respectively.

$$\begin{bmatrix} v_1 \\ v_2 \\ \vdots \\ v_l \end{bmatrix} = \begin{bmatrix} \sin\frac{\pi x_1}{L} & \sin\frac{2\pi x_1}{L} & \cdots & \sin\frac{n\pi x_1}{L} \\ \sin\frac{\pi x_2}{L} & \sin\frac{2\pi x_2}{L} & \cdots & \sin\frac{n\pi x_2}{L} \\ \vdots & \vdots & \vdots & \vdots \\ \sin\frac{\pi x_l}{L} & \sin\frac{2\pi x_l}{L} & \cdots & \sin\frac{n\pi x_l}{L} \end{bmatrix}\begin{bmatrix} V_1 \\ V_2 \\ \vdots \\ V_n \end{bmatrix}, \quad (6)$$

$$\begin{bmatrix} \ddot{v}_1 \\ \ddot{v}_2 \\ \vdots \\ \ddot{v}_l \end{bmatrix} = \begin{bmatrix} \sin\dfrac{\pi x_1}{L} & \sin\dfrac{2\pi x_1}{L} & \cdots & \sin\dfrac{n\pi x_1}{L} \\ \sin\dfrac{\pi x_2}{L} & \sin\dfrac{2\pi x_2}{L} & \cdots & \sin\dfrac{n\pi x_2}{L} \\ \vdots & \vdots & \vdots & \vdots \\ \sin\dfrac{\pi x_l}{L} & \sin\dfrac{2\pi x_l}{L} & \cdots & \sin\dfrac{n\pi x_l}{L} \end{bmatrix} \begin{bmatrix} \ddot{V}_1 \\ \ddot{V}_2 \\ \vdots \\ \ddot{V}_n \end{bmatrix}. \tag{7}$$

Similarly, using the relationship $M = -EI(\partial^2 v/\partial x^2)$, the bending moments at the corresponding locations can also be obtained as:

$$\begin{bmatrix} M_1 \\ M_2 \\ \vdots \\ M_l \end{bmatrix} = -EI\frac{\pi^2}{L^2} \begin{bmatrix} \sin\dfrac{\pi x_1}{L} & 2^2\sin\dfrac{2\pi x_1}{L} & \cdots & n^2\sin\dfrac{n\pi x_1}{L} \\ \sin\dfrac{\pi x_2}{L} & 2^2\sin\dfrac{2\pi x_2}{L} & \cdots & n^2\sin\dfrac{n\pi x_2}{L} \\ \vdots & \vdots & \vdots & \vdots \\ \sin\dfrac{\pi x_l}{L} & 2^2\sin\dfrac{2\pi x_l}{L} & \cdots & n^2\sin\dfrac{n\pi x_l}{L} \end{bmatrix} \begin{bmatrix} V_1 \\ V_2 \\ \vdots \\ V_n \end{bmatrix}. \tag{8}$$

## 2.2. INTERPRETING CONSTANT MOVING LOADS

If $P_1, P_2, \ldots, P_k$ are constant moving loads and ignoring the effect of damping, the closed form solution of equation (1) is given as:

$$v(x,t) = \frac{L^3}{48EI}\sum_{i=1}^{k} P_i \sum_{j=1}^{\infty} \frac{1}{j^2(j^2-\alpha^2)} \sin\frac{j\pi x}{L}\left(\sin\frac{j\pi(ct-\hat{x}_i)}{L} - \frac{\alpha}{j}\sin\omega_{(j)}(t-\hat{x}_i/c)\right), \tag{9}$$

in which $\alpha = \pi c/L\omega_{(1)}$.

Therefore, if the displacements of the beam at $x_1, x_2, \ldots, x_l$ caused by a set of constant moving loads are known, the magnitude of each moving load can be obtained by solving the following equation.

$$\{v\} = [S_{vP}]\{P\}, \tag{10}$$

in which $\{v\} = [v_1\ v_2\ \cdots\ v_l]^T$, $\{P\} = [P_1\ P_2\ \cdots\ P_k]$ and

$$[S_{vp}] = \begin{bmatrix} s_{11} & \cdots & \cdots & \cdots & s_{1k} \\ \vdots & \ddots & & & \vdots \\ s_{m1} & & s_{mi} & & s_{mk} \\ \vdots & & & \ddots & \vdots \\ s_{11} & \cdots & \cdots & \cdots & s_{lk} \end{bmatrix}, \tag{11}$$

where

$$s_{mi} = \frac{L^3}{48EI} \sum_{j=1}^{\infty} \frac{1}{j^2(j^2 - \alpha^2)} \sin\frac{j\pi x_m}{L} \left( \sin\frac{j\pi(ct - \hat{x}_i)}{L} - \frac{\alpha}{j} \sin\omega_{(j)}(t - \hat{x}_i/c) \right). \quad (12)$$

If $l \geqslant k$, which means the number of displacement measuring stations is larger than or equal to the number of axle loads, $\{P\}$ can be derived by the following equation:

$$\{P\} = ([S_{vP}]^T[S_{vP}])^{-1}[S_{vP}]^T\{v\}. \quad (13)$$

The least square estimate of $\{P\}$ can be obtained by referring to the work of Leon [25]. A similar equation can be obtained for using bending moments instead of displacements as the bridge responses by considering the closed form solution in terms of bending moments.

$$M(x, t) = \frac{L}{4} \sum_{i=1}^{k} P_i \sum_{j=1}^{\infty} \frac{8j^2}{\pi^2} \sin\frac{j\pi x}{L} \frac{1}{j^2(j^2 - \alpha^2)} \left[ \sin\frac{j\pi(ct - \hat{x}_i)}{L} - \frac{\alpha}{j} \sin\omega_{(j)} \left( t - \frac{\hat{x}_i}{c} \right) \right]. \quad (14)$$

It is noted that if the set of moving loads consists of time-varying loads, the method can still be applied to determine their static equivalent values as other traditional weigh-in-motion methods.

### 2.3. INTERPRETING TIME-VARYING MOVING LOADS

The above mentioned method can also be applied to interpret moving time-varying axle loads. At first the bridge responses at various locations, such as the vertical displacements or bending moments, are transformed to modal values using equations (6) and (8) respectively. The central difference method is used to numerically differentiate the modal displacements to obtain the corresponding modal velocities and modal accelerations. Then equation (4) becomes a set of linear equations in which the values of the axle load at any instant, i.e., $P_1, P_2, \ldots, P_k$, can be solved by the least squares method.

## 3. DYNAMIC INTERACTIVE FORCES FOR A TWO-AXLE VEHICLE MODEL

A two-axle vehicle model is developed to generate the theoretical responses and the corresponding interactive moving forces. The theoretical responses are then used as the input data for the interpretive method to "interpret" the interactive forces. The interpreted interactive moving forces are then compared with the interactive forces from the two-axle vehicle model and this can serve as an independent check of the interpretive method.

Consider a simple two-axle vehicle model, as shown in Figure 2. The vehicle is symmetrical about its centre-line and with a mass $M_v$. The equations of motion of the vehicle are expressed as

$$M_v\ddot{y} = C_v(\dot{v}_2 - \dot{y}_2 + \dot{v}_1 - \dot{y}_1) + K_v(v_2 - y_2 + v_1 - y_1) + K_v(r_1 + r_2), \quad (15)$$

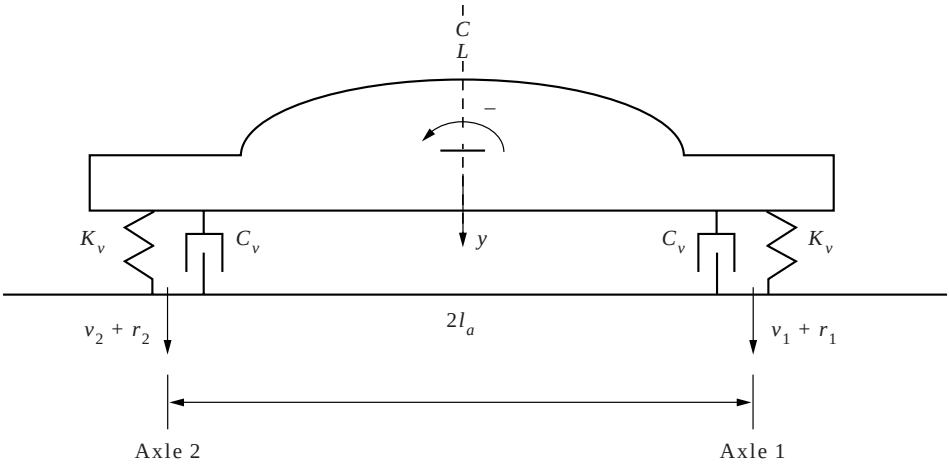


Figure 2. A simple two-axle vehicle model.

$$J\ddot{\theta} = C_v l_a(\dot{v}_2 - \dot{y} - \dot{v}_1 + \dot{y}_1) + K_v l_a(v_2 - y_2 - v_1 + y_1) + K_v l_a(-r_1 + r_2), \quad (16)$$

where $y_i$, and $r_i$ are the $i$th axle vertical displacement and road surface roughness respectively; $K_v$ and $C_v$ are the spring stiffness and damping ratio of the axles; $J$ is the radius of gyration of the vehicle; $2l_a$ is the axle spacing and $v_i$ is the vertical displacement of the bridge under the $i$th axle, in which

$$v_i = \sum_{j=1}^{n} \sin\frac{j\pi(ct - \hat{x}_i)}{L} V_j = \sum_{j=1}^{n} S_{ji} V_j \qquad i = 1, 2. \quad (17)$$

$V_j$ ($j = 1, 2, \ldots$) are the modal displacements and $\hat{x}_i$ is the distance of the $i$th axle with respect to the first axle.

Substituting $y_1 = y - l_a\theta$, $y_2 = y + l_a\theta$ and applying the above equation, equations (15) and (16) can be re-written as,

$$M_v\ddot{y} + 2C_v\dot{y} + 2K_v y - C_v\left(\sum_{j=1}^{n} S_{j1}\dot{V}_1 + \sum_{j=1}^{n} S_{j2}\dot{V}_2\right) - K_v\left(\sum_{j=1}^{n} S_{j1}V_1 + \sum_{j=1}^{n} S_{j2}V_2\right)$$

$$= K_v(r_1 + r_2), \quad (18)$$

$$J\ddot{\theta} + 2l_a^2 C_v\dot{\theta} + 2l_a^2 K_v\theta + C_v l_a\left(\sum_{j=1}^{n} S_{j1}\dot{V}_1 - \sum_{j=1}^{n} S_{j2}\dot{V}_2\right) + K_v l_a\left(\sum_{j=1}^{n} S_{j1}V_1\right.$$

$$\left. - \sum_{j=1}^{n} S_{j2}V_2\right) = K_v l_a(r_2 - r_1). \quad (19)$$

Now considering the relative displacement and relative velocity of each axle with respect to the bridge deck, the interactive force at the $i$th axle is expressed as follows:

$$P_i = K_v\left(y - l_a\theta - \sum_{j=1}^{n} S_{ji}V_j\right) + C_v\left(\dot{y} - l_a\dot{\theta} - \sum_{j=1}^{n} S_{ji}V_j\right) - K_v r_i + W_i, \qquad (20)$$

where $W_i$ $(i = 1, 2)$ are the axle weights of the vehicle.

Substituting equation (20) into equation (4) gives

$$\begin{aligned}
&\ddot{V}_m + 2\zeta_m\omega_m\dot{V}_m + \omega_m^2 V_m \\
&= \frac{2}{\mu L}\left\{S_{m1}K_v\left(y - l_a\theta - \sum_{j=1}^{n} S_{j1}V_j\right) + S_{m1}C_v\left(\dot{y} - l_a\dot{\theta} - \sum_{j=1}^{n} S_{j1}\dot{V}_j\right)\right. \\
&+ S_{m2}K_v\left(y + l_a\theta - \sum_{j=1}^{n} S_{j2}V_j\right) + S_{m2}C_v\left(\dot{y} + l_a\dot{\theta} - \sum_{j=1}^{n} S_{j2}\dot{V}_j\right) \\
&\left. - S_{m1}K_v r_1 - S_{m2}K_v r_2 + S_{m1}W_1 + S_{m2}W_2\right\}. \qquad (21)
\end{aligned}$$

Hence, the coupled vibration equation of the vehicle-bridge system is expressed as follows:

$$\begin{bmatrix}[M_{nn}] & [M_{nc}] \\ [M_{cn}] & [M_{cc}]\end{bmatrix}\begin{bmatrix}\{\ddot{V}\} \\ \{\ddot{Y}\}\end{bmatrix} + \begin{bmatrix}[C_{nn}] & [C_{nc}] \\ [C_{cn}] & [C_{cc}]\end{bmatrix}\begin{bmatrix}\{\dot{V}\} \\ \{\dot{Y}\}\end{bmatrix} + \begin{bmatrix}K_{nn}] & [K_{nc}] \\ [K_{cn}] & [K_{cc}]\end{bmatrix}\begin{bmatrix}\{V\} \\ \{Y\}\end{bmatrix} = \begin{bmatrix}\{R_n\} \\ \{R_c\}\end{bmatrix}, \qquad (22)$$

where expressions for each parameter are given in Appendix A.

Equation (22) can be solved by any direct integration method. In the present study, the Newmark $\beta$ method is adopted. From the nodal displacements, velocities and accelerations obtained, equations (6) to (8) can be used to obtain the displacements, accelerations and bending moments of the bridge at various locations.

Based on the work of O'Connor and Chan [15], a computer program VBRIAN—an acronym derived from Vehicle-BRidge Interaction ANalysis, was developed for the above mentioned two-axle vehicle model. The case with two constant loads running across a beam at constant velocity was compared with the closed form solution given by equation (9) and it was found that the two sets of results were identical.

## 4. EXAMPLE OF A BRIDGE–VEHICLE SYSTEM

Figures 3–6 show the dynamic response given by the program VBRIAN for the case when a two-axle vehicle proceeds at 20 m/s across a full-scale bridge

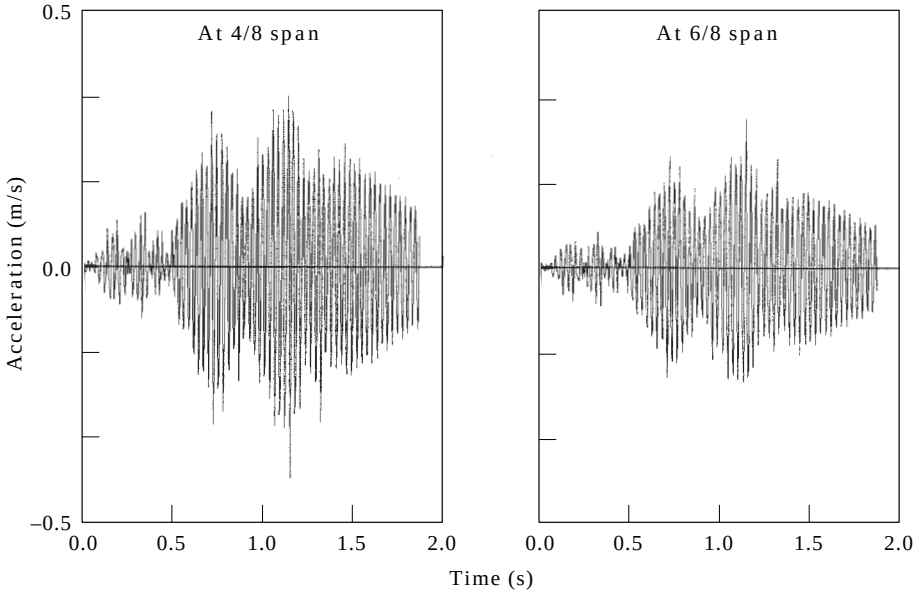


Figure 3. Acceleration at mid-span and 3/4-span.

with a span of 27·4 m. The quantities used in the calculation are tabulated in Table 1.

The data above were chosen with reference to the practical ranges of bridge and vehicle parameters, as defined by Chan and Chan [26]. Figure 3 shows the responses of acceleration at middle and three-quarter-spans. Figures 4 and 5 show the time histories of the displacements and bending moments, respectively, at the seven measurement locations.

## 5. METHOD VALIDATION

A computer program LOADID, an acronym derived from LOAD IDentification, was written based on equation (4) to identify the interactive force of the bridge–vehicle system using the corresponding responses, e.g., bending

TABLE 1

*Summary of the bridge and vehicle parameters*

| Bridge parameters | | Vehicle parameters | |
|---|---|---|---|
| Number of modes | 3 | $K_v$ | 128·5 kN/m |
| No. of measurement locations | 7 | $C_v$ | 998·65 N/ms |
| $EI$ | 26 581 MN m$^2$ | $M_v$ | 8613·5 kg |
| $\mu$ | 6067 kg/m | $J$ | 11 484·67 kg m$^2$ |
| $L$ | 27·4 m | $c$ | 20 m/s |
| | | $l_a$ | 2 m |

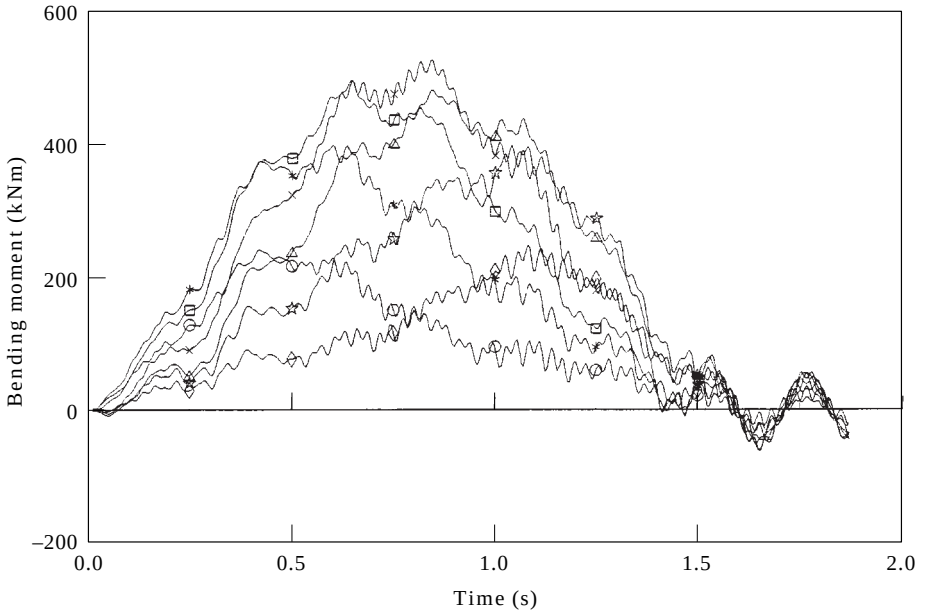


Figure 4. Time history of displacement: ○, at 1/8 span; ∗, at 2/8 span; □, at 3/8 span; ×, at 4/8 span; △, at 5/8 span; ★, at 6/8 span; ◇, at 7/8 span.

moments or displacements, as generated from the VBRIAN program. Then the interactive forces from VBRIAN are compared with the identified interactive force from LOADID. The bridge responses acquired in the field usually contain

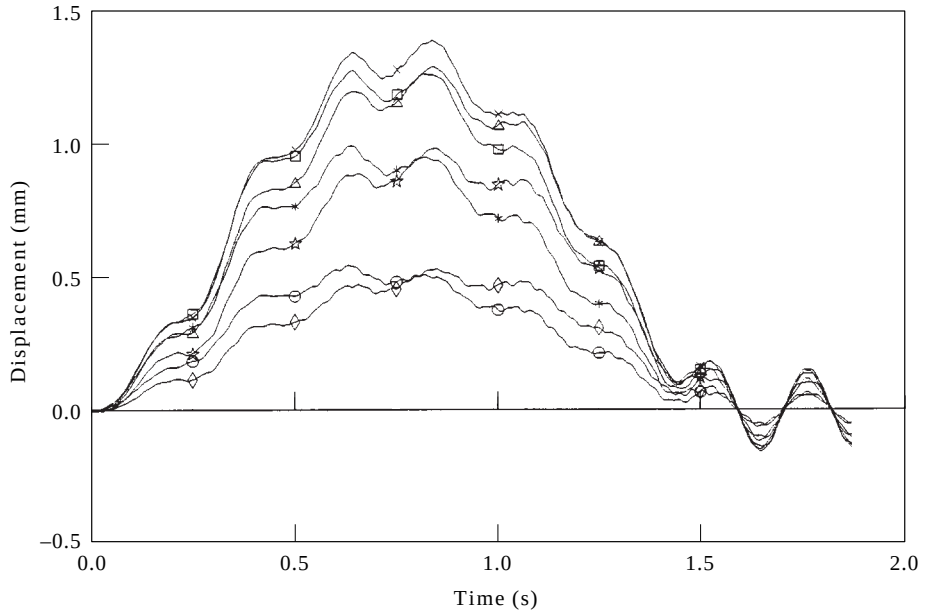


Figure 5. Time history of bending moment. Key as for Figure 4.

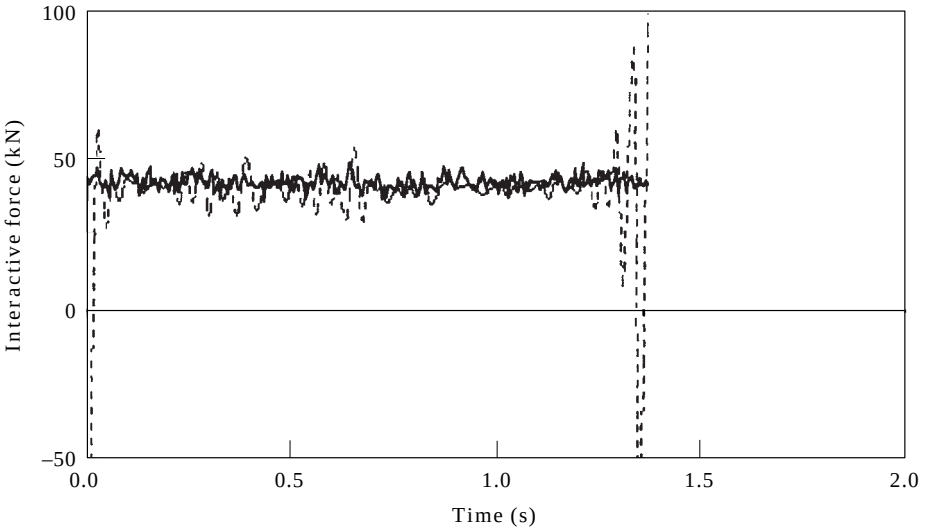


Figure 6. Interactive force for axle 1: true (solid) and identified (dashed).

measurement noise. Therefore, white noise was added to the calculated responses to simulate the polluted measurements.

$$Data_{input} = Data_{generated}(1 + E_p \times N_{oise}), \tag{23}$$

where $E_p$ is a specified error level; $N_{oise}$ is a standard normal distribution random data with zero mean value and unity standard deviation.

When $E_p = 0$, i.e., where no noises are added into the generated responses, the two sets of results are identical. This means the proposed method is correct. When $E_p = 1$, a filtering scheme of the polluted data has to be included in the identified procedures. A low-pass filter with 10% width of original frequency band, which

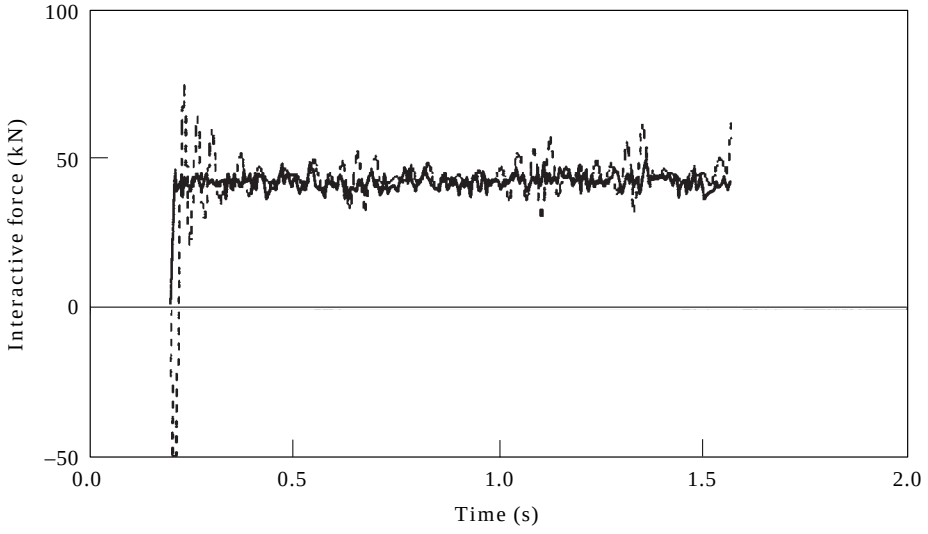


Figure 7. Interactive force for axle 2: true (solid) and identified (dashed).

is about 300 Hz for this case, is used for the filtering of the polluted data. Figures 6 and 7 show the results of the identified interactive forces (dash lines) using bending moment as the input responses for the first and second axles compared with the corresponding interactive forces (solid lines) generated from the bridge–vehicle system described in the example. The interactive forces are also identified using displacements, and the results of identification using bending moment are much better than those using displacement.

It is interesting to substitute the identified interactive forces in equation (4) to calculate the modal displacements and use equation (8) to generate the corresponding (rebuilt) bending moments caused by the identified forces. Figure 8 shows the reconstructed mid-span bending moment compared with the original bending moment from VBRIAN. It can be seen that the two sets of bending moment agree quite well indicating an accurate identification of the interactive forces using the proposed method.

## 6. ERROR STUDIES

Further studies were carried out to study the sensitivity of predicted loads to errors in the measurement. The simulated measurements were again polluted by adding random errors and equation (23) was used to generate the polluted measurements. A low pass filter with 10% width of the original frequency was again used to filter the polluted data. Error levels 1%, 2% and 5%, i.e., $E_p = 1$, 2 and 5, were included in the study. The axle spacing adopted in the last example was 4 m. It is interesting to know how the accuracy of the identified forces was affected by changing the value of axle spacing. Table 1 shows the identification error of the identified force of the two axles with respect to various

TABLE 2

*Identification error for span = 27·4 m*

| | Identification error (%) | | | | | |
|---|---|---|---|---|---|---|
| | Axle 1 | | | Axle 2 | | |
| Axle spacing (m) | $E_p = 1$ | $E_p = 2$ | $E_p = 5$ | $E_p = 1$ | $E_p = 2$ | $E_p = 5$ |
| 2 | 23·78 (9200) | 30·86 (16 782) | 58·23 (36 810) | 16·42 (8940) | 41·91 (15 457) | 63·88 (37 200) |
| 4 | 12·58 (3987) | 13·65 (7245) | 27·85 (16 773) | 11·44 (3669) | 18·19 (8874) | 43·70 (20 115) |
| 8 | 6·43 (1534) | 7·89 (3116) | 12·98 (8144) | 3·29 (1710) | 5·00 (3442) | 9·68 (8797) |

error levels and axle spacings. The identification error is given by the following equation:

$$\text{Identification error (\%)} = \frac{\sum_{j=1}^{n} |\text{Identified force}_j - \text{Generated interactive force}_j|}{\sum_{j=1}^{n} |\text{Generated interactive force}_j|} * 100\%, \quad (24)$$

where $n$ is the total number of time steps. The generated interactive force is the corresponding interactive force from the bridge–vehicle system that generated the measured responses for the identification.

A similar study was carried out for a bridge span of 10 m. Results in Tables 2 and 3 show that the identification errors increase by increasing the noise level. Besides, results in Tables 2 and 3 show that the identification errors decrease by decreasing axle spacing of vehicles. An axle-spacing-to-span ratio (ASR) is defined as the ratio of the axle spacing between two consecutive axles of a vehicle to the bridge span length. If ASR is small, the two closely spaced axles are hard to identify individually and large identification errors will be produced. Relatively, for vehicles on short-span bridges, ASR is large and therefore two axles would well be identified.

Figure 6 shows two sudden changes separately at the beginning and end of the time history which correspond to the time when the second axle entering and the first axle is leaving the bridge. These two sudden changes are due to the coefficients in the first matrix on the right hand side of equation (4) being very small, and so extremely large values would be obtained after the inversion of the matrix to obtain the interactive forces. Similar results are obtained for the second axle, as shown in Figure 7.

TABLE 3

*Identificatioin error for span = 10 m*

| | Identification error (%) | | | | | |
|---|---|---|---|---|---|---|
| | Axle 1 | | | Axle 2 | | |
| Axle spacing (m) | $E_p = 1$ | $E_p = 2$ | $E_p = 5$ | $E_p = 1$ | $E_p = 2$ | $E_p = 5$ |
| 2 | 2·42 (42·31) | 2·32 (65·30) | 2·18 (199·81) | 2·31 (49·50) | 2·57 (77·45) | 2·47 (179·55) |
| 4 | 1·05 (31·45) | 1·25 (60·98) | 1·57 (142·13) | 1·21 (31·40) | 1·26 (62·76) | 1·54 (144·66) |
| 8 | 1·52 (16·56) | 1·64 (31·15) | 1·93 (72·91) | 1·56 (15·81) | 1·59 (31·38) | 1·80 (74·07) |

Values in brackets are identification errors of unfiltered interactive forces.

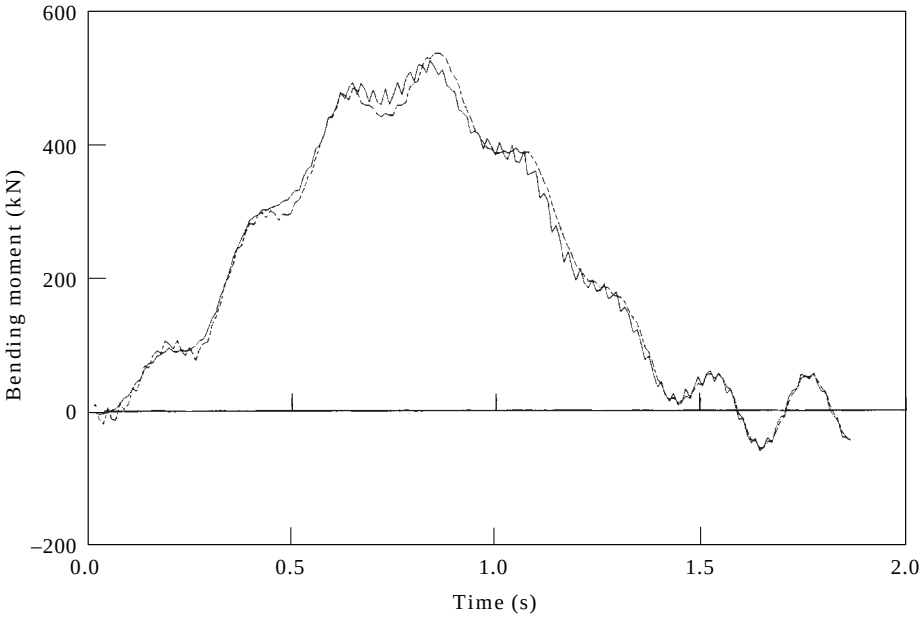


Figure 8. Rebuilt (dotted) and original (solid) mid-span bending moment.

Bridge responses induced by vehicles running over a road with road surface roughness would be equal to the bridge responses induced by vehicles running over a smooth road surface with a certain level of noise [27]. The level is normally less than 13% for poor road condition [28]. Based on the present study, the method could give acceptable results with such a level of noise.

## 7. MULTI-AXLE IDENTIFICATION

In order to study the accuracy of the method for multi-axle identification, three-axle and four-axle loading models were used (Figure 9). Table 4 shows the

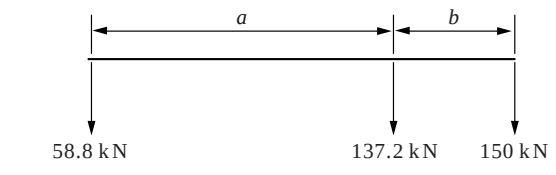


(a)

| Case | *a*(m) | *b*(m) |
|---|---|---|
| 1 | 3.0 | 2.5 |
| 2 | 3.4 | 1.6 |
| 3 | 3.5 | 1.3 |

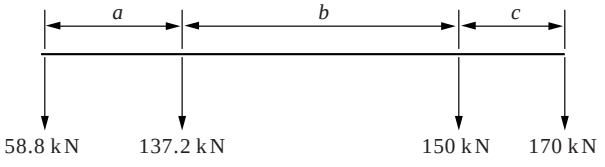


(b)

| Case | *a*(m) | *b*(m) | *c*(m) |
|---|---|---|---|
| 1 | 2.0 | 6.0 | 1.5 |
| 2 | 2.5 | 4.0 | 1.5 |
| 3 | 3.0 | 4.0 | 1.3 |

Figure 9. Configuration of the three-axle (a) and the four-axle (b) vehicle models.

TABLE 4

*Percentage errors of some exaples of multi-axle force identification*

| Span | Speed | SF (Hz) | Mode and sensor no. | a* | b* | c* | Axle 1 (%) | Axle 2 (%) | Axle 3 (%) | Axle 4 (%) |
|---|---|---|---|---|---|---|---|---|---|---|
| 50 | 10 | 1000 | 7 | 2·0 | – | – | 4·8 | 1·7 | – | – |
| 45 | 10·5 | 1000 | 9 | 3·5 | 4·8 | – | 5·7 | 4·1 | 6·4 | – |
| 40 | 11 | 500 | 13 | 2·5 | 6·5 | 8·0 | 2·4 | 0·5 | 1·3 | 1·6 |
| 35 | 11·5 | 500 | 7 | 3·5 | – | – | 1·4 | 0·5 | – | – |
| 30 | 12 | 1000 | 7 | 3·4 | 5·0 | – | 3·3 | 0·9 | 1·5 | – |
| 25 | 12·5 | 1000 | 7 | 3·0 | 7·0 | 8·3 | 1·6 | 0·5 | 1·0 | 1·3 |
| 20 | 13 | 500 | 7 | 6·0 | – | – | 1·2 | 0·8 | – | – |
| 15 | 13·5 | 1000 | 7 | 3·0 | 5·5 | – | 0·7 | 0·4 | 0·4 | – |
| 10 | 14 | 2000 | 7 | 2·0 | 8·0 | 9·5 | 0·4 | 0·4 | 0·6 | 0·3 |

*Please refer to Figure 9 for definition of a, b and c.

TABLE 5

*Recommended number of strain gauges*

| $\sigma$ | No. of strain gauges |
|---|---|
| $\leqslant 0{\cdot}333$ | 7 |
| $0{\cdot}37 \sim 0{\cdot}50$ | 9 |
| $0{\cdot}615 \sim 1{\cdot}124$ | 13 |
| $\geqslant 1{\cdot}124$ | N/A |

percentage errors for this study and it is shown that the method is applicable to multi-axle identification.

## 8. RECOMMENDED NUMBER OF SENSORS

The accuracy of the predicted loads will also depend on the number of sensors. An identification parameter is defined to study this accuracy.

$$\sigma = \frac{c}{f} * \frac{1}{ASR}, \tag{25}$$

where $f$ is the sampling frequency. Based on studying cases using different span lengths, speeds of vehicles, ASRs, sampling frequencies and number of strain gauges, the recommended number of strain gauges for various identification parameters are given in Table 5. It is also found that the method is valid to identify moving axle forces when $\sigma$ is less than 1·124.

## 9. PRACTICAL SIGNIFICANCE

From the above study, it can be seen that the accuracy of identification depends on the length of bridge span and axle spacing. Shorter spans and larger axle spacings will give greater accuracy in the identification. Table 2 shows that the identification error is always less than 5% for the case of 10 m span. For a span of 27·4 m, an axle spacing less than 4 m always has an identification error greater than 10%. Therefore, the method can be used to identify the interactive force of a vehicle with an axle spacing greater than 4 m. It would be difficult to identify

TABLE 6

*Typical axle spacings of heavy vehicles*

| Vehicle type | a* | b* | c* | Gross weight (tonnes) |
|---|---|---|---|---|
| Diesel truck | 6·02 | 1·30 | – | 24·5 |
| Concrete mixer | 3·35 | 1·30 | – | 24·0 |
| Trailer | 3·40 | 4·50 | 1·24 | 31·5 |

* Please refer to Figure 9 for definition of a, b and c.

individual axle loads within tandem or tri-axle groups. Table 6 shows typical axle spacing of heavy vehicles. Based on a detailed study of the dynamic effect caused by these two groups, Chan and O'Connor [29] concluded that, in the study of the dynamic behaviour of bridge–vehicle interaction, the axles within a group, tandem or tri-axle, can be replaced by an equivalent single axle acting at the centre of the group. Therefore, the method can still be applied to identify the interactive force of a vehicle with tandem or tri-axle groups.

For the above study, the speed and number of axles of vehicles are given. To study the proposed method using field data, bridge and vehicle parameters are prerequisite. The dynamic properties of a test bridge can be obtained from a modal test. Bridge responses can be measured using strain gauges. The measured responses are then converted to nodal displacements as input data. The vehicle parameters can be measured using two axle sensors. The two axle sensors are installed on the road surface of the test bridge. The speed of vehicles can be calculated by dividing the distance between the two axle sensors by the time taken by an axle passing the two axle sensors. The axle spacing of vehicles can be obtained by counting the number of sudden changes measured using the axle sensor. The axle spacing of vehicles can be measured by multiplying the speed by the time taken by a vehicle passing the axle sensor.

## 10. CONCLUSIONS

A method to identify constant/equivalent static and time-varying axle loads using bridge responses is proposed. A bridge–vehicle system is developed to generate the bridge responses and the corresponding interactive force. The study suggests the following conclusions: (1) It is feasible to use bridge responses to identify moving constant/equivalent static or time-varying axle loads. (2) The bridge responses used can be bending moment as obtained from strain gauges, and displacement as obtained from linear transducers. (3) Accurate results of identified force can be obtained with no noise added to the generated input data. (4) A filtering scheme is required to smooth the polluted data in order to obtain acceptable results. (5) Identification using bending moment will give better results compared with using displacement. (6) Shorter spans or larger axle spacings will give greater accuracy in the identification. The identification error is always less than 5% for the case of 10 m span, and for a span of 27·4 m, the identification error is always greater than 10% for an axle spacing less than 4 m. (7) The number of sensors used depends on the values of identification parameter $\sigma$ and the method cannot be applied to a case if $\sigma$ is greater than 1·124.

To conclude, a feasible method to identify moving loads, including time-varying and equivalent static loads, has been developed.

## ACKNOWLEDGMENT

The present project supported by the Hong Kong Research Grants Council.

## REFERENCES


1. F. Moses 1978 *Transportation Research Board Transportation Research Record* **664**, 198–206. Reliability approaches to bridge safety and truck loading uncertainties.
2. F. Moses 1979 *Transactions of Transportation Engineering Journal of ASCE* **105** (TE3), 233–249. Weigh-in-motion system using instrumented bridges.
3. J. H. Daniels, J. L. Wilson, B. T. Yen, L. Y. Lai and R. Abbaszadeh 1986 *Proceedings of 3rd Annual International Bridge Conference*, 136–142. WIM plus response study of four in-service bridges.
4. P. Davis and F. Sommerville 1987 *Transportation Research Record* **1123**, 122–126. Calibration and accuracy testing of weigh-in-motion systems.
5. D. M. Freund and R. F. Bonaquist 1989 *Public Roads* **52**, 97–106. Evaluation of a weigh-in-motion device at the pavement testing facility.
6. S. Gassner, K. Overlach, H. Kauer and J. Madek 1986 *SAE Technical Paper Series Paper* 861104. Current research efforts in weigh in motion.
7. R. J. Peters 1984 *Proceedings of 12th ARRB Conference* **2**, 10–18. AXWAY—a system to obtain vehicle axle weights.
8. R. J. Peters 1986 *Proceedings of 13th ARRB and 5th REAAA Combined Conference* **6**, 70–83. CULWAY—an unmanned and undetectable highway speed vehicle weighing system.
9. B. A. Jacob 1994 *Proceedings of NATDAC* '94. European Research Activity COST 323—Weigh-in-motion of road vehicles.
10. B. A. Jacob and E. J. O'Brien 1996 *National Traffic Data Acquisition Conference* (*NATDAQ* '96), 659–668. WAVE—a European research project on weigh-in-motion.
11. T. H. T. Chan 1988 *PhD Thesis*, *University of Queensland*, *Australia*. Highway bridge impact.
12. D. Cebon 1987 *Symposium on Heavy Vehicle Suspension and Characteristics*, *Australian Road Research Board*. Assessment of the dynamic wheel forces generated by heavy road vehicles.
13. A. P. Whittemore, J. R. Wiley, P. C. Schultz and D. E. Pollock 1970 *Highway Research Board*, *National Cooperative Highway Research Program Report No*. 105. Dynamic pavement loads of heavy highway vehicles.
14. R. Cantieni 1992 *Swiss Federal Laboratories for Materials Testing and Research* (*EMPA*) *Report No*. 220. Dynamic behaviour of highway bridges under the passage of heavy vehicles.
15. C. O'Connor and T. H. T. Chan 1988 *Journal of Structural Engineering ASCE* **114**, 1703–1723. Dynamic loads from bridge strains.
16. S. S. Law, T. H. T. Chan and Q. H. Zeng 1997 *Journal of Sound and Vibration* **201**, 1–22. Moving force identification—time domain method.
17. S. S. Law, T. H. T. Chan and Q. H. Zeng *Journal of Dynamic Systems*, *Measurement and Control ASME* (accepted for publication). Moving force identification—frequency domain method.
18. R. S. Ayre, G. Ford and L. S. Jacobson 1950 *Journal of Applied Mechanics ASME* **72**, 283–290. Transverse vibration of a two-span bridge under action of a moving constant force.
19. E. Saibel and W. F. Z. Lee 1952 *Journal of the Franklin Institute* **254**, 499–516. Vibration of a continuous beam under a constant moving force.
20. M. M. Stanisic and J. C. Hardin 1969 *Journal of Franklin Institute* **287**, 115–123. On the response of beams to an arbitrary number of concentrated moving masses.
21. A. Kaplan, N. Lipner, F. B. Robert and R. O. Strom 1970 Report No. *FRA-RT*-70-23, prepared for OHSGT, US Department of Transportation under Contract No. C-353-66. Train elevated guideway interactions.
22. N. Lipner, D. A. Evensen and A. Kaplan 1970 Report No. FRA-RT-71-42, Volumes 1 and 2, TRW Systems Group, Redondo Beach, CA. Dynamic response of continuous beam elevated guideway.

23. R. W. TRENSE and L. VAN DER GRAFF 1974 *Ingenier* **76**, C1–B8. The calculation of girder bridges for moving loads.
24. L. FRYBA 1972 *Vibration of Solids and Structures under Moving Loads*. Noordhoff International Publishing, Prague.
25. S. J. LEON 1994 *Linear Algebra with Application*. Macmillan College Publishing Company, Inc, New York.
26. T. H. T. CHAN and H. F. CHAN 1996 *Proceedings of Highway into the Next Century Conference*, *Hong Kong*, 169–176. Parametric studies on highway bridge impact.
27. M. J. INBANATHAN and M. WIELAND 1987 *Journal of Structural Engineering ASCE* **113**, 1994–2008. Bridge vibration due to vehicle moving over rough surface.
28. H. M. METWALLY, F. K. SALMAN and A. M. EL LAKANY 1993 *Proceedings of the* 11*th International Modal Analysis Conference*, 1564–1571. An improved matrix method for the dynamic response for modelling structure under moving vehicles.
29. T. H. T. CHAN and C. O'CONNOR 1990 *Journal of Structural Engineering* **116**, 1772–1793. Vehicle model for highway bridge impact.

## APPENDIX A: EXPRESSION FOR VARIOUS PARAMETERS IN EQUATION

$$[M_{nc}] = [0] \quad [M_{cn}] = 0 \quad [M_{nn}] = \begin{bmatrix} 1 & & 0 \\ & \ddots & \\ 0 & & 1 \end{bmatrix} \quad [M_{cc}] = \begin{bmatrix} M_v & 0 \\ 0 & J \end{bmatrix},$$

Appendix A—(*Continued overleaf*)

$$[C_{nn}] = \begin{bmatrix} 2\zeta_1\omega_1 + \frac{2}{\mu L} C_v(S_{11}^2 + S_{12}^2) & \frac{2}{\mu L} C_v(S_{11}S_{21} + S_{12}S_{22}) & \cdots & \frac{2}{\mu L} C_v(S_{11}S_{n1} + S_{12}S_{n2}) \\ \frac{2}{\mu L} C_v(S_{21}S_{11} + S_{22}S_{12}) & 2\zeta_2\omega_2 + \frac{2}{\mu L} C_v(S_{21}^2 + S_{22}^2) & \cdots & \frac{2}{\mu L} C_v(S_{21}S_{n1} + S_{22}S_{n2}) \\ \vdots & \vdots & \vdots & \vdots \\ \frac{2}{\mu L} C_v(S_{n1}S_{11} + S_{n2}S_{12}) & \frac{2}{\mu L} C_v(S_{n1}S_{21} + S_{n2}S_{22}) & \cdots & 2\zeta_n\omega_n + \frac{2}{\mu L} C_v(S_{n1}^2 + S_{12}^2) \end{bmatrix},$$

$$[C_{cn}] = \begin{bmatrix} -C_v(S_{11} + S_{12}) & -C_v(S_{21} + S_{22}) & \cdots & -C_v(S_{n1} + S_{n2}) \\ C_v l_a(S_{11} - S_{12}) & C_v l_a(S_{21} - S_{22}) & \cdots & C_v l_a(S_{n1} - S_{n2}) \end{bmatrix},$$

$$[C_{cc}] = \begin{bmatrix} 2C_v & 0 \\ 0 & 2C_v l_a^2 \end{bmatrix},$$

$$[C_{nc}] = \begin{bmatrix} -\frac{2}{\mu L} C_v(S_{11} + S_{12}) & \frac{2}{\mu L} C_v l_a(S_{11} - S_{12}) \\ -\frac{2}{\mu L} C_v(S_{21} + S_{22}) & \frac{2}{\mu L} C_v l_a(S_{21} - S_{22}) \\ \vdots & \vdots \\ -\frac{2}{\mu L} C_v(S_{n1} + S_{n2}) & \frac{2}{\mu L} C_v l_a(S_{n1} - S_{n2}) \end{bmatrix},$$

$$[K_{nn}] = \begin{bmatrix} \omega_1^2 + \frac{2}{\mu L} K_v(S_{11}^2 + S_{12}^2) & \frac{2}{\mu L} K_v(S_{11}S_{21} + S_{12}S_{22}) & \cdots & \frac{2}{\mu L} K_v(S_{11}S_{n1} + S_{12}S_{n2}) \\ \frac{2}{\mu L} K_v(S_{21}S_{11} + S_{22}S_{12}) & \omega_2^2 + \frac{2}{\mu L} K_v(S_{21}^2 + S_{22}^2) & \cdots & \frac{2}{\mu L} K_v(S_{21}S_{n1} + S_{22}S_{n2}) \\ \vdots & \vdots & \vdots & \vdots \\ \frac{2}{\mu L} K_v(S_{n1}S_{11} + S_{n2}S_{12}) & \frac{2}{\mu L} K_v(S_{n1}S_{21} + S_{n2}S_{22}) & \cdots & \omega_n^2 + \frac{2}{\mu L} K_v(S_{n1}^2 + S_{n2}^2) \end{bmatrix},$$

$$[K_{cn}] = \begin{bmatrix} -K_v(S_{11}+S_{12}) & -K_v(S_{21}+S_{22}) & \cdots & -K_v(S_{n1}+S_{n2}) \\ K_v l_a(S_{11}-S_{12}) & K_v l_a(S_{21}-S_{22}) & \cdots & K_v l_a(S_{n1}-S_{n2}) \end{bmatrix},$$

$$[K_{cc}] = \begin{bmatrix} 2K_v & 0 \\ 0 & 2K_v l_a^2 \end{bmatrix},$$

$$[K_{nc}] = \begin{bmatrix} -\frac{2}{\mu L}K_v(S_{11}+S_{12}) & \frac{2}{\mu L}K_v l_a(S_{11}-S_{12}) \\ -\frac{2}{\mu L}K_v(S_{21}+S_{22}) & \frac{2}{\mu L}K_v l_a(S_{21}-S_{22}) \\ \vdots & \vdots \\ -\frac{2}{\mu L}K_v(S_{n1}+S_{n2}) & \frac{2}{\mu L}K_v l_a(S_{n1}-S_{n2}) \end{bmatrix},$$

$$\{R_n\} = \begin{bmatrix} -\frac{2}{\mu L}K_v(S_{11}r_1+S_{12}r_2)+\frac{2}{\mu L}(S_{11}W_1+S_{12}W_2) \\ -\frac{2}{\mu L}K_v(S_{21}r_1+S_{22}r_2)+\frac{2}{\mu L}(S_{21}W_1+S_{22}W_2) \\ \vdots \\ -\frac{2}{\mu L}K_v(S_{n1}r_1+S_{n2}r_2)+\frac{2}{\mu L}(S_nW_1+S_{n2}W_2) \end{bmatrix},$$

$$\{R_c\} = \begin{bmatrix} K_v(r_1+r_2) \\ K_v l_a(r_2-r_1) \end{bmatrix},$$

$$\{V\} = \begin{bmatrix} V_1 \\ V_2 \\ \vdots \\ V_n \end{bmatrix}, \qquad \{Y\} = \begin{bmatrix} y \\ \theta \end{bmatrix},$$

## APPENDIX B: NOTATION

| | |
|---|---|
| $\dot{\cdot}$ | first time derivative, i.e., velocity |
| $\ddot{\cdot}$ | second time derivative, i.e., acceleration |
| $A$ | axle spacing |
| $c$ | speed of the moving load |
| $C$ | viscous damping ratio |
| $C_v$ | axle viscous damping ratio |
| $E$ | Young's modulus |
| $E_P$ | error level |
| $f$ | sampling frequency |
| $I$ | second moment of area |

$J$ radius of gyration of the vehicle model
$K_v$ axle stiffness
$l_a$ half of the vehicle axle spacing
$L$ span length
$M$ bending moment
$M_v$ mass of the vehicle model
$P$ moving load
$r_i$ road surface roughness under $i$th axle
$v$ beam deflections
$v_i$ beam deflections under $i$th axle
$V$ modal displacements
$W_i$ weight of $i$th axle
$\hat{x}_k$ distance between the $k$th and 1st loads
$y$ vertical displacement of the vehicle model
$y_i$ $i$th axle vertical displacement
$Y$ vector containing vertical $y$ and $\theta$
$\delta(x)$ the Dirac function
$\mu$ mass per unit length
$\theta$ angular rotation of the vehicle model
$\omega_{(j)}$ angular frequency at $j$th mode
$\zeta_{(j)}$ angular damping ratio at $j$th mode